Available online at www.sciencedirect.com

SciVerse ScienceDirect

Journal of Nutritional Biochemistry 23 (2012) 1285–1293

Journal of Nutritional Biochemistry

HuR-mediated posttranscriptional regulation of p21 is involved in the effect of *Glycyrrhiza uralensis* licorice aqueous extract on polyamine-depleted intestinal crypt cells proliferation

Yi He[a,b,1], Xian Zhang[a,1], Xing Zeng[a,*], Yu Huang[a], Jian-An Wei[a], Ling Han[a], Cai-Xia Li[a], Guo-Wei Zhang[a]

[a]Central Laboratory of the Second Affiliated Hospital, Guangzhou University of Chinese Medicine, Guangzhou 510120, P.R. China
[b]The First Affiliated Hospital of Guangxi Traditional Chinese Medical College, Nanning 530023, P.R. China

Received 24 February 2011; received in revised form 17 May 2011; accepted 26 July 2011

Abstract

Glycyrrhiza uralensis licorice has long been used worldwide as a food additive and herbal medicine. It possesses a remarkable healing action on gastrointestinal ulcers. The present study was carried out to assess the effect of licorice on intestinal crypt cell proliferation and to investigate the corresponding molecular mechanism. Considering the role of crypt stem cells in intestinal mucosa repair, a well-established cytostatic cellular model, polyamine-depleted IEC-6 cells, was utilized to evaluate the effect of aqueous licorice on the proliferation of intestinal crypt cells. The growth inhibition of IEC-6 cells caused by alpha-difluoromethylornithine could be significantly reversed by concomitant treatment with 40 μg/ml and 80 μg/ml licorice aqueous extract. In particular, the restoration of cell cycle progression was accompanied by a decrease in p21 mRNA level and cytoplasmic accumulation of the RNA-binding protein HuR, which was shown to be involved in the destabilization of p21 mRNA. Using a biotin pull-down assay and a luciferase assay, it was found that licorice-modulated p21 mRNA expression was achieved by HuR-targeted AU-rich and U-rich elements that resided in the 3′ untranslated region of p21 mRNA. These results demonstrate that licorice can exert its action on stimulating the growth of intestinal crypt cells by regulating p21 mRNA level at the posttranscriptional level by HuR.

Keywords: *Glycyrrhiza uralensis* licorice; Intestinal crypt cells; Cell proliferation; Cyclin-dependent kinase inhibitor p21; HuR; Posttranscriptional regulation

1. Introduction

Licorice, which means “sweet root” in Greek, has long been used as a food additive due to its sweet flavor. Moreover, it has been used worldwide for thousand of years as a remedy for many ailments [1,2]. Its extract and derivatives have been reported to exert a healing effect on a variety of epithelial injuries, such as gastric and duodenal ulcers [3], aphthous ulcers [4], dermal wounds [5] and urogenital ulcers [1]. The most predominant and constant medicinal use for licorice has been as an antipeptic ulcer drug because the licorice extract was recommended as a remedy for peptic ulcer by Revers in 1946 [6]. It is postulated that the ulcer-healing properties of licorice partly lie in the stimulation of mucus synthesis [7–9].

The intestinal epithelium sustains injury in response to stresses ranging from physiologic daily digestive trauma to severe insults associated with ischemia, chemicals, infection and radiation [10]. As the most rapidly renewing tissue in adult mammals, the small intestinal epithelium achieves its continual replenishment by stem cells that reside in the crypts of small intestine and differentiate into other types of enterocytes [11,12]. The healing of lesions after intestinal injuries is sequentially accomplished by migration, proliferation and differentiation of intestinal crypt cells [13]. Therefore, the rapid proliferation of intestinal crypt cells plays a major role in maintaining the integrity and barrier function of intestinal mucosa under physiological and pathological conditions.

A 3-(4,5-dimethylthiazol-2-yl)-2,5-diphenyltetrazolium bromide assay previously conducted by other investigators showed that licorice extract stimulates the proliferation of a normal intestinal epithelial crypt cell line, IEC-6 [14]. Although it has not been confirmed by additional experiments, this preliminary finding suggests that intestinal crypt cells may be a potential target for licorice-mediated intestinal healing. How licorice promotes the proliferation of intestine crypt cells still remains elusive.

The IEC-6 cell line is one of the most accessible models appropriate for studying the proliferation of intestinal crypt cells [15]. A well-

Abbreviations: 3′F, a HuR-targeted sequence in p21 mRNA 3′-UTR; AREs, AU-rich elements; DAPI, 4′,6-diamidino-2-phenylindole; DFMO, alpha-difluoromethylornithine; CR, coding region; FCM, flow cytometry; GC, Gan Cao granules; GA, glycyrrhizic acid monoammonium salt; HPLC, high-performance liquid chromatography; LQ, liquiritin; mRNP, messenger ribonucleoprotein; PBS, phosphate-buffered saline; qRT-PCR, quantitative real-time polymerase chain reaction; RBPs, RNA-binding proteins; TCM, traditional Chinese medicine; UTR, untranslated region.

* Corresponding author. Tel.: +86 2039318678; fax: +86 2039318678.
E-mail address: zengxing-china@163.com (X. Zeng).

[1] Yi He and Xian Zhang contributed equal to this work.

0955-2863/$ - see front matter.
doi:10.1016/j.jnutbio.2011.07.009

established pathological cellular model for studying cell proliferation under growth arrest status is induced by alpha-difluoromethylornithine (DFMO), which acts as a highly specific inhibitor of amino-acid-derived polyamine biosynthesis and retards cell growth and mucosal repair in rats with stress ulcers [16–18]. This pathological cellular model contributes substantially to a lot of regulatory factors in the proliferation of intestinal cells, such as p21, p27, p53 [19], c-fos, c-myc, c-jun [20], junD [21] and TGF-beta [22]. With increasing awareness of the important role of posttranscriptional events in regulating gene expression in eukaryotes [23], it has been discovered that certain RNA binding proteins (RBPs) influence the biogenesis, stability, function, transport and cellular localization of mRNAs [24]. Previous studies have shown that the mRNA levels of p53, NPM, junD and TGF-beta are associated with the mRNA stability of these genes during the proliferation of IEC-6 cells [21,22,25], in which cytoplasmic accumulation of a ubiquitously expressed RBP, HuR, was involved [26]. HuR specifically binds to mRNAs containing AU-rich elements (AREs) in their 3′ untranslated regions (3′-UTR) [27]. These HuR-targeted mRNAs include cyclin A, cyclin B1 [28], c-myc [29], p53 [30] and p21 [31].

Therefore, the aim of this work was to determine whether licorice is effective in stimulating the proliferation of the intestinal crypt cell line IEC-6 under pathological conditions and explore the possible molecular mechanism at the posttranscriptional level. Using the cell growth inhibition cellular model induced by DFMO, we narrowed our focus to the role of HuR in regulating one of its target mRNAs, the cyclin-dependent kinase inhibitor p21.

2. Materials and methods

2.1. Aqueous extract of licorice

The aqueous extract powder of *Glycyrrhiza uralensis* licorice, Gan Cao in Chinese, used in this study has the commercial name Gan Cao Granules (GC) (Lot No. 08021800) and was obtained from the Jiangyin Tianjiang Pharmaceutical Co., Ltd. (Jiangsu, China). According to the manufacturer, 0.5 g of concentrated powder is equivalent to approximately 3 g of crude plant extract. To ensure the identity of GC in each cell culture treatment, the same batch of GC was used for all experiments.

2.2. High-performance liquid chromatography (HPLC)-based quality control

Prior to all experiments, quality control was performed with regard to the properties of GC. According to the official method described by the *Pharmacopoeia of the People's Republic of China* [32], the quality control of GC was conducted as follows. HPLC analysis was performed on a Shimadzu LC-10AT system (Kyoto, Japan) using a Shimadzu C18 reversed-phase column (5 μm particle size, 250×4.6 mm i.d.) at 25°C. Two major marker components, glycyrrhizic acid monoammonium salt (GA) and liquiritin (LQ), were obtained from the National Institute for the Control of Pharmaceutical and Biological Products (Beijing, P.R. China). Initially, the GC samples were separately dissolved in the appropriate mobile phase solution for eluting GA and LQ, sonicated for 30 min and filtered with 0.45-μm pore size membrane filters (Millipore, Bedford, MA, USA). The injection volume was 10 μl, and the flow rate was 1 ml/min. GA was isocratically eluted using a mobile phase containing methanol/0.2 M ammonium acetate/acetic acid (67:33:1) at a flow rate of 1 ml/min and detected at 250 nm. LQ was eluted with isocratic acetonitrile/0.5% acetic acid at a flow rate of 1 ml/min and detected at 276 nm. The concentration of GA and LQ in GC was measured according to the respective standard curves (peak area vs. concentration) and assayed in triplicate.

2.3. Cell culture and experimental treatment

The IEC-6 cell line, which was derived from normal rat small intestinal crypts and maintained the characteristics of nontransformed crypt epithelial cells, was purchased from American Type Culture Collection (Manassas, VA, USA.) at passage 14. Passages 15–20 were used in our experiments, and the cells were maintained at a constant growth rate and cell morphology approximately until the 20th passage. All cell culture vessels were purchased from Greiner Bio-one (Frickenhausen, Germany). IEC-6 cells were routinely maintained in Dulbecco's modified Eagle's medium (GIBCO, Gaithersburg, MD, USA) supplemented with 5% heat-inactivated fetal bovine serum (Thermo Scientific HyClone, Logan, UT, USA), 10 μg/ml bovine insulin (Sigma-Aldrich, St. Louis, MO, USA) and 50 μg/ml gentamicin sulfate (GIBCO, Gaithersburg, MD, USA) at 37°C in 5% CO_2–95% air. DFMO was obtained from Hangzhou Rongda Pharm & Chem Co, Ltd. (Hangzhou, P.R. China). At the initiation of all experiments, cells were seeded in cell culture dishes at a density of 2×10^3 cells/cm^2. After complete attachment, control cells were cultured in normal DMEM medium. DFMO-treated cells were grown in normal medium plus 5 mM DFMO. IEC-6 cells treated with DFMO and GC were cultured in normal medium supplemented with 5 mM DFMO plus 40 μg/ml GC or 80 μg/ml GC. The medium was changed every other day [19].

2.4. Cell number measurement

IEC-6 cells were seeded in 60-mm-diameter dishes and were continuously subjected to drug treatment for 6 days. Every other day during this period, the cells were harvested with trypsin-EDTA (GIBCO, Gaithersburg, MD, USA) and washed with phosphate-buffered saline (PBS) buffer (Thermo Scientific HyClone, Logan, UT, USA). Following resuspension in PBS buffer to a concentration of at least 1×10^5 cells/ml, the cells were counted using Cell Lab Quanta SC MPL flow cytometry (Beckman Coulter, Fullerton, CA, USA).

2.5. Cell cycle analysis

The cellular DNA content was measured by staining with 4′,6-diamidino-2-phenylindole (DAPI). IEC-6 cells were collected by trypsinization and washing with PBS. The cell pellets were added to 10 μg/ml DAPI (NPE Systems Inc., Pembroke Pines, FL, USA) to obtain a final cell concentration of $1–2\times10^6$ cells/ml. After incubation for 10 min at room temperature, the samples were run using Cell Lab Quanta SC MPL flow cytometry (FCM). The DNA content histograms were calculated by Phoenix MultiCycle AV software (Phoenix Flow Systems, San Diego, CA, USA).

2.6. Quantitative real-time polymerase chain reaction (qRT-PCR) analysis

Total RNA was extracted from cultures using TRIzol reagent (Invitrogen, Carlsbad, CA, USA). An aliquot of 1 μg of RNA was reverse transcribed into a single-strand cDNA with the Reverse Transcription System (Promega, Madison, WI, USA). The sequences of the specific primer pairs of target gene p21 were as follows: sense, 5′-CAAAGTATGCCGTCGTCTGT-3′ and antisense, 5′-GTCTCAGTGGCGAAGTCAAA-3′. An internal housekeeping gene control, beta-actin, was used to normalize the initial calculation of total RNA. The sequences of beta-actin primer pairs were as follows: sense, 5′-CCCATCTATGAGGGTTACGC-3′ and antisense, 5′-TTTAATGTCACGCACGATTTC-3′. Quantitative RT-PCR was performed using the ABI 7500 real-time PCR system (Applied Biosystems, Foster City, CA, USA) and the RT-PCR reagent SYBR Premix *Ex Taq* II (TaKaRa, Dalian, China.). The strategy for analyzing relative gene expression was the $2^{-\Delta\Delta Ct}$ method.

2.7. mRNA stability analysis

The half-life of p21 mRNA was determined by treating IEC-6 cells with actinomycin D (Sigma Chemical Co., St. Louis, MO, USA), as described by Zou et al. [33]. Briefly, IEC-6 cells were cultured under experimental condition for 6 days and then underwent *de novo* incubation with 5 μg/ml actinomycin D to block mRNA transcription. During the subsequent 10 h, cells were harvested at 0, 2, 4, 6 and 10 h. Total RNA was extracted and qRT-PCR was performed as described in the previous section.

2.8. Western blot analysis

Whole-cell lysates were prepared using RIPA buffer (Pierce, Rockford, IL, USA). Cytoplasmic and nuclear proteins were fractionally extracted with NE-PER Nuclear and Cytoplasmic Extraction Reagents (Thermo Scientific, Rockford, IL, USA). Meanwhile, complete protease inhibitor cocktail tablets (Roche, Indianapolis, IN, USA) were added to the extraction reagent above to protect proteins from degradation. After measuring protein concentration with the BCA method, an equal amount of denatured proteins were subjected to sodium dodecyl sulfate polyacrylamide gel electrophoresis using 12% or 15% polyacrylamide gels [34]. After transferring to polyvinylidene fluoride membranes, the proteins were, respectively, probed with specific primary antibodies recognizing p21 (BD Pharmingen, San Diego, CA, USA), HuR (Santa Cruz Biotechnology, Inc., Santa Cruz, CA, USA), beta-actin (KangChen Bio-tech, Shanghai, China), alpha-tubulin (Santa Cruz Biotechnology, Inc., Santa Cruz, CA, USA) and Lamin B1 (Santa Cruz Biotechnology, Inc., Santa Cruz, CA, USA), incubated with the appropriate secondary antibodies (Jackson ImmunoResearch Laboratories, Inc., West Grove, PA, USA) and visualized with ECL substrate.

2.9. Immunoprecipitation of messenger ribonucleoprotein (mRNP) complexes

To isolate mRNAs from endogenously formed mRNP complexes and identify the interaction of HuR and p21 mRNA, immunoprecipitation of mRNP complexes was performed as described [35]. Briefly, mRNP complex-containing lysates were prepared from 75×10^6 freshly cultured cells per sample, and the supernatant of the lysate was precleared using Protein A-Sepharose beads and an IgG1 antibody. Antibody-immobilized Protein A-Sepharose beads were prepared by incubation with anti-HuR and IgG1 overnight and mixed with the mRNP lysates at room temperature. After extracting mRNA from mRNP complexes, the presence of endogenous HuR associated-mRNAs was identified by RT-PCR, and the PCR products were visualized by electrophoresis using 2% agarose stained with the fluorescent nucleic acid GelRed (Biotium, Hayward, CA, USA).

2.10. Synthesis of biotinylated transcripts and biotin pull-down assay

Rattus norvegicus p21 mRNA (NM_080782.3) was predicted to have several HuR binding sites in its 3′-UTR, which contains AREs and U-rich elements. For the *in vitro* synthesis of biotinylated transcripts, total RNA from IEC-6 cells was reverse transcribed, and the cDNAs were used as templates for amplifying the 5′-UTR, coding region (CR), 3′-UTR and the representative sequence containing the predicted HuR motif hit in the 3′-UTR (3′F) of p21 mRNA. With the T7 polymerase promoter sequence (T7) 5′-TAATACGACTCACTATAGGGAGA-3′ at the 5′-end, the sequence of the 5′-UTR was synthesized directly as (T7) 5′-GGGATGCATCTATCTTGTGATATGTACCAGCCA-CAGGCACC-3′. For CR, 3′-UTR and 3′F, the 5′ primers also contained T7 RNA polymerase promoter sequences. The sequences of primer pairs used to synthesize the DNA template of CR are as follows: (T7) 5′-ATGTCCGATCCTGGTGATGT-3′ and 5′-TCAGGGCTTTCTCTTGCAG-3′. The primers pairs (T7) 5′-AGTGCCCACGGGAGGCTC-3′ and 5′-CAGCTTGGGTTGAGAAGGAC-3′ were prepared for the oligonucleotides of the 3′-UTR. Similarly, (T7) 5′-AGTGCCCACGGGAGGCTC-3′ and 5′-CAGCTTGGGTTGAGAAG-GAC-3′ were used as the primers for the 3′F. Specific PCR-amplified transcripts with the T7 promoter were purified from agarose gels with the Wizard SV Gel and PCR Clean-Up System (Promega, Madison, WI, USA) and used as templates for synthesizing the corresponding biotinylated RNA using T7 polymerase (MEGAscript T7 kit, Ambion, Austin, TX, USA) and biotin-CTP (Enzo Life Science, Farmingdale, NY, USA). Prior to the following procedure, the biotin-RNA probes were purified using NucAway spin columns (Ambion, Austin, TX, USA). The biotin pull-down assay was carried out by incubating 6 μg of the biotin RNA-probe with 120 μg of cytoplasmic lysates for 30 min at room temperature. RNA-binding proteins were extracted using streptavidin-conjugated Dynabeads (Dynal, Oslo, Norway) and magnetic separation and were analyzed by western blot.

2.11. Reporter plasmids and dual-luciferase reporter assays

To construct a reporter plasmid containing the ARE fragment from the p21 mRNA 3′ UTR, the corresponding dsDNA of 3′F (mentioned in the biotin pull-down assay) was amplified using IEC-6 cDNA and the following specific primer pairs with an *Xba*I restriction site: sense, 5′-GCTCTAGAAGTGCCCACGGGAGGCTC-3′ and antisense, 5′-GCTCTAGACAGCTTGGGTTGAGAAGGAC-3′ (restriction sites underlined). The PCR product was cloned into the pGL3-Promoter Vector (Promega, Madison, WI, USA) at the *Xba*I site, downstream of the luciferase gene, to generate the chimeric pGL3-Luc-3′F. The fidelity and orientation of the fragment in the luciferase reporter were confirmed by DNA sequencing and enzyme digestion. Different groups of cells were grown in 24-well plates for 72 h and then cotransfected with pGL3-Promoter Vector plus pRL-SV40 Vector or pGL3-Luc-3′F plasmid plus pRL-SV40 Vector using Lipofectamine 2000 (Invitrogen, Carlsbad, CA, USA). pRL-SV40 Vector (Promega, Madison, WI, USA) carrying the Renilla luciferase reporter gene served as an internal control for normalizing the transfection efficiency. After 6 h of incubation, the transfection solution was replaced with fresh medium. Luciferase activity was measured using the Dual-Luciferase Reporter Assay System (Promega, Madison, WI, USA) after 48 h of transfection.

2.12. Statistics

All values were from at least triplicate samples and expressed as means±standard error of the mean (S.E.M.). Experiments were repeated three times. The statistics package SPSS 15.0 for Windows was used for the statistical analysis. Differences in the variables among the groups were compared by one-way analysis of variance followed by post hoc tests to determine the level of significance. A P value<.05 was considered statistically significant.

3. Results

3.1. HPLC analysis

Glycyrrhizic acid and LQ are established as the two major marker compounds in the *Pharmacopoeia of the People's Republic of China* for the quality control of licorice. The national criteria state that the amounts of glycyrrhizic acid and LQ in crude licorice, which are detected separately by HPLC, should be no less than 2% and 1%, respectively. As reported in the "Materials and Methods" section, the percentage (% w/w) of glycyrrhizic acid and LQ in the GC was determined to be 6.11%±0.22% and 3.77%±0.26%, respectively. The HPLC profiles are shown in the Supplemental Data.

3.2. Effect of GC on cell proliferation and cell cycle progression of DFMO-treated IEC-6 cells

The DFMO-induced growth retardation *in vitro* model was employed to test our hypothesis that GC might regulate the proliferation of intestinal crypt cells under growth inhibition. Cells were seeded at an initial density of 2×10^3 cells/cm^2 and routinely observed every day. After 6 days of treatment, compared to the control cells, the growth inhibition in the DFMO-treated cells was visualized by microscopy, and the growth inhibition seemed to be reversed by supplementing with 40 μg/ml and 80 μg/ml GC. Moreover, the second dose appeared to be more effective than the first one when comparing the confluence of the cells (Fig. 1A). This interesting phenomenon was further evaluated quantitatively through the following FCM-based experiments for assessing proliferative capacity.

First, simultaneous and direct measurement of cell number and viability was performed using flow cytometry with an integrated Coulter counter (Beckman Cell Lab Quanta SC). Corresponding exactly to the results of the microscopic observation, the cell count in the group supplemented with 40 μg/ml GC and 80 μg/ml GC was noticeably elevated on the sixth day of treatment (Fig. 1B).

Second, cell cycle analysis via DAPI staining provided further proof for cell proliferation. Similar to the results reported by others [19], cell cycle progression in DFMO-treated cells was arrested by polyamine depletion compared to normal cells. In Fig. 2A, compared to the control group, cells in S and G2/M phase were decreased after 6 days of DFMO treatment. However, supplementation with 40 μg/ml and 80 μg/ml GC increased the number of cells in S phase and G2/M phase. Accordingly, the proliferation indices of the cells exposed to 40 μg/ml and 80 μg/ml GC were elevated compared to control cells (Fig. 2B). These results indicate that GC plays a role in promoting the cell cycle progression of DFMO-treated IEC-6 cells to return to normal.

3.3. GC reversed DFMO-induced increases in p21 expression and mRNA stability

p21, a cyclin-dependent kinase inhibitor, plays a key role in regulating the cell cycle by interacting with cyclin–CDK complexes and directly inhibiting their kinase activity [36]. Previous studies have shown that the inhibition of cell growth induced by DFMO is accompanied by an increase in p21 expression [19,37]. Thus, we assumed that the changes in p21 expression might be a possible mechanism by which GC rescues the growth arrest induced by DFMO. In Fig. 3A, after 6 days of treatment, p21 mRNA level increased in the DFMO-treated cells approximately 10-fold compared to the control cells; in contrast, p21 mRNA in cells treated with DFMO plus 40 μg/ml or 80 μg/ml GC was down-regulated remarkably. Accordingly, the dramatic expression of p21 protein raised under polyamine deprivation conditions was also depressed in the cells treated with 40 μg/ml or 80 μg/ml GC (Fig. 3B and C). These findings might shed light on the phenomenon discovered by FCM, as mentioned above. Therefore, we further investigated the possible posttranscriptional mechanism by which GC regulates the expression of p21 mRNA in polyamine-depleted IEC-6 cells.

Numerous studies have shown that mRNA stability plays an important role in the posttranscriptional regulation of gene expression [38]. To discover the intrinsic mechanism of GC in modulating p21 mRNA expression, we focused our research on whether GC is involved in regulating p21 mRNA stability in DFMO-treated IEC-6 cells. In Fig. 4, p21 mRNA stability in cells treated with DFMO was greatly enhanced compared to normal cells at each time point during the period of transcriptional blocking. In contrast, the presence of 40 μg/ml or 80 μg/ml GC reduced the elevated p21 mRNA stability caused by DFMO to the normal level. These results suggest that the effect of GC on p21 mRNA expression is associated with its role in destabilizing p21 mRNA.

3.4. GC regulates the nucleocytoplasmic distribution of HuR in IEC-6 cells

The findings of p21 mRNA destabilization after GC treatment led us to narrow our focus to HuR, a RNA-binding protein that stabilizes mRNA though its cytoplasmic translocation [25,28]. In the present

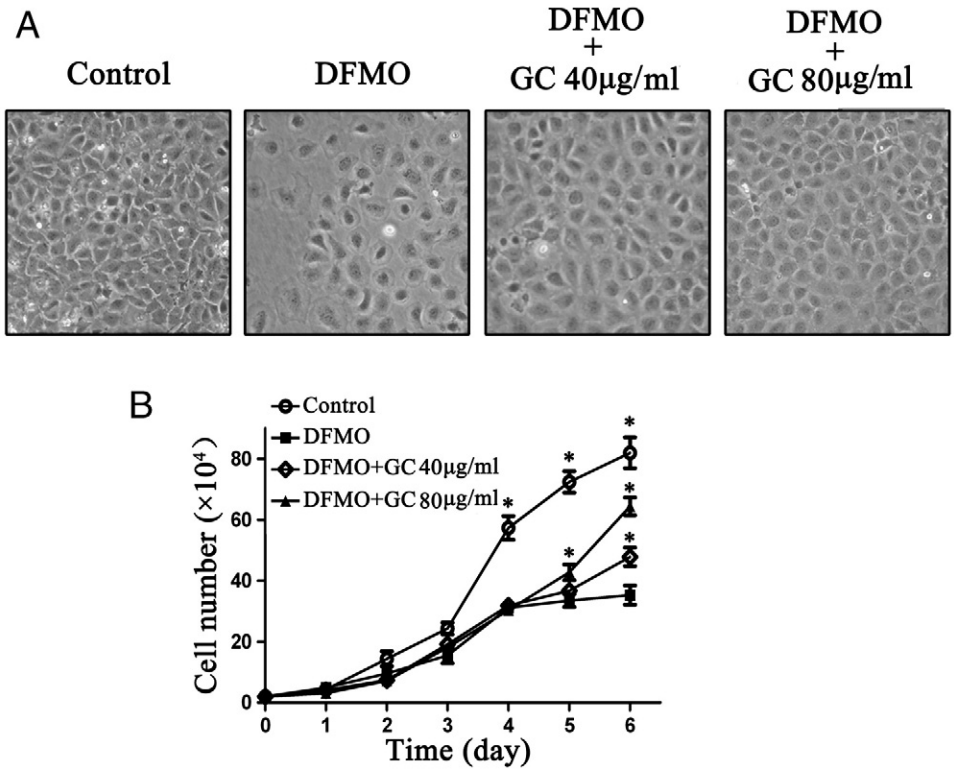

Fig. 1. Microscopic images and growth curve after treatment. (A) After a 6-day treatment, the changes in cell density in the different groups were visualized under a Nikon microscope at a magnification of 100×. (B) The growth curve displays the absolute counts of cells cultured in 60-mm dishes during the 6-day treatment. The data at each time point are from three independent experiments with triplicate samples per group. *P<.05 when compared to cells treated with DFMO.

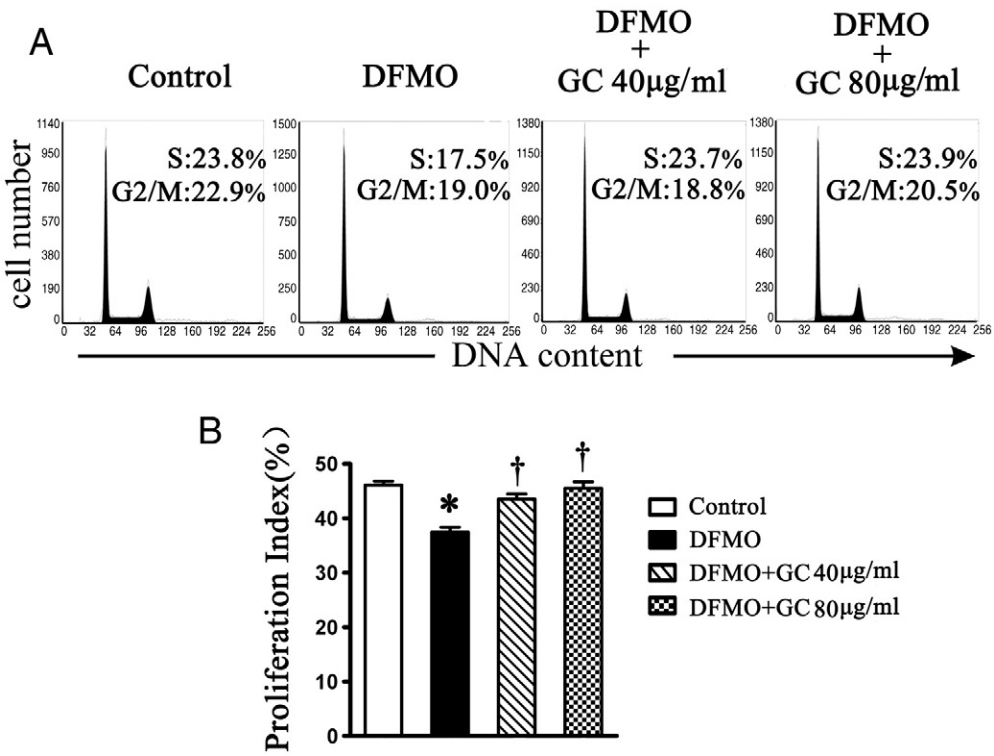

Fig. 2. Cell cycle analysis by flow cytometry. (A) The histograms represent 10,000 events. The abscissa represents the corresponding DNA content. The left peak depicts the amount of cells in G0/G1 phase, the peak on the right displays the ratio of the cells in G2/M phase, and the area between both peaks depicts the amount of cells fraction residing in S phase. (B) Based on the percentage of cells in each cell cycle phase (G0/G1, S and G2/M), the proliferation index was calculated through the proliferation index formula [100%×(S+G2/M)/(G0/G1 +S+G2/M)]. Values are the mean±S.E.M. of data from three independent experiments. *P<.05 when compared to control cells and cells treated with DFMO plus GC. †P<.05 when compared to cells treated with DFMO.

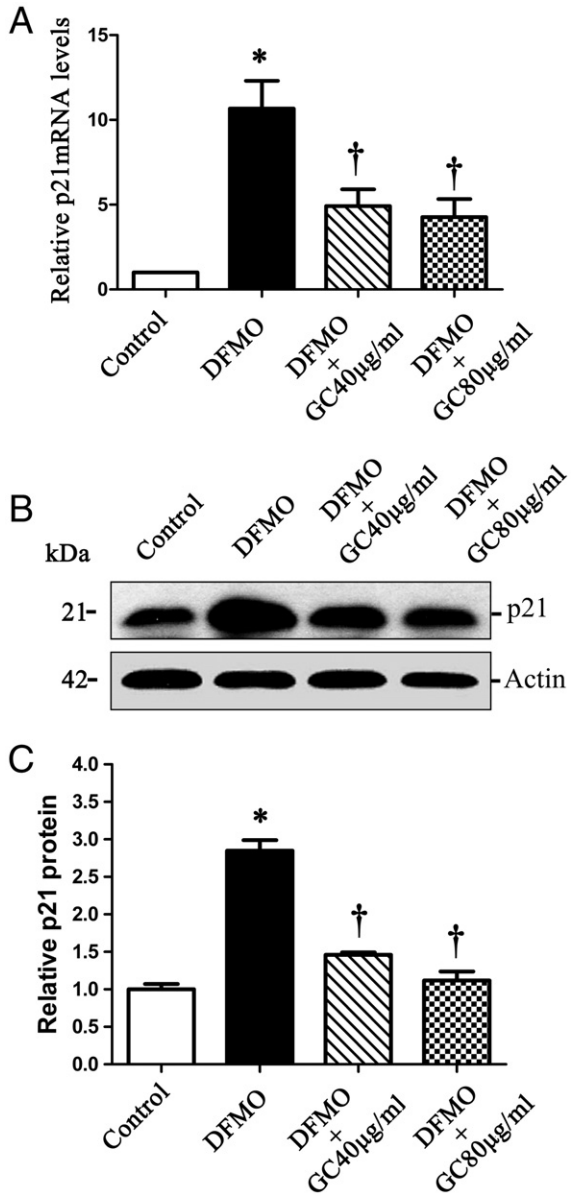

Fig. 3. Changes in p21 gene expression at the transcriptional and translational levels. (A) Relative p21 mRNA levels measured by qRT-PCR. Values are the mean±S.E.M. of data from three independent experiments. *P<.05 when compared to control cells and cells treated with DFMO plus GC. †P<.05 when compared to cells treated with DFMO. (B) Representative western blots detecting p21 protein in the whole-cell lysate. Eighty micrograms of total protein was loaded in each lane. Immunoblots were probed with a p21-specific antibody (21 kDa). Beta-actin served as the loading control (42 kDa). (C) Quantitative analysis derived from densitometric scans of immunoblots of total p21 as described for (B). Values are the mean±S.E.M. from three separate experiments. *P<.05 when compared to controls and cells treated with DFMO plus GC. †P<.05 when compared to cells treated with DFMO.

study, the cytoplasmic and nuclear HuR in IEC-6 cells treated with DFMO plus 40 μg/ml or 80 μg/ml GC was distributed in a way opposite to the nucleocytoplasmic abundance of HuR in DFMO-treated cells (Fig. 5A, B and C). In other words, HuR in the GC groups remained more in the nuclei compared to the DFMO-treated cells. No contamination occurred between the proteins in both the cytoplasmic and nuclear fractions (Fig. 5A, lamin B1; Fig. 5B, alpha-tubulin). Total HuR remained unchanged in the different groups, which indicates that it did not contribute to the subcellular distribution of HuR (Fig. 5C). This finding is consistent with the result of the mRNA stability analysis and implies that the relative stagnation of HuR in nuclei may

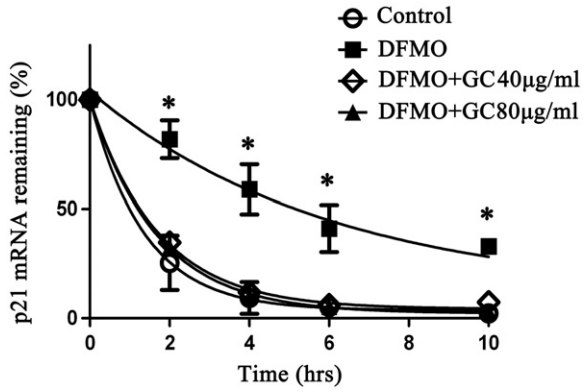

Fig. 4. Effect of GC on p21 mRNA stability. The levels of p21 mRNA at the indicated time points were determined by qRT-PCR and represented as the remaining percentage of initial mRNA level. Values are the mean±S.E.M. of data from three independent experiments. *P<.05 when compared to control cells and cells maintained in DFMO plus 40 μg/ml or 80 μg/ml GC.

partially account for the destabilization of p21 mRNA when treated with GC.

3.5. GC regulates the interaction between cytoplasmic HuR and p21 mRNA

It has been reported that HuR stabilizes its target mRNAs by binding their AU-rich and U-rich elements to form HuR–mRNA complexes (mRNPs) and exporting them together from the nucleus to the cytoplasm [39]. To further identify whether the effect of GC on p21 mRNA stability and HuR nuclear-cytoplasmic shuttling is associated with the increased cytoplasmic accumulation of the HuR–p21 mRNP complex, endogenous HuR–mRNA complexes from cytoplasmic protein lysate were immunoprecipitated with HuR-specific antibody, and the mRNA components binding to HuR were isolated and amplified with reverse transcription PCR using specific primer pairs for p21 (see "Materials and Methods"). p21 mRNA in endogenous HuR-mRNPs from the cytoplasmic compartment increased significantly in the presence of DFMO (Fig. 6A and B), and the interaction between p21 mRNA and HuR was partially inhibited in the HuR–mRNP complexes from cells treated with 40 μg/ml or 80 μg/ml GC. As a control, p21 mRNA was undetectable in nonspecific IgG1 immunoprecipitates (Fig. 6A, right). Considering the regulatory role of HuR on p21 mRNA stability [31], this result supports the fact that the effect of GC on the binding affinity of HuR and p21mRNA might play a role in modulating p21 expression.

3.6. The effect of GC on p21 expression is associated with the HuR-targeted ARE from the p21 mRNA 3′-UTR

Based on the finding that GC affected the cytoplasmic translocation of HuR-p21 mRNP, two experiments were conducted to further investigate whether AU-rich and U-rich elements in p21 mRNA were the targets of GC regulation.

First, we performed a search of AREs in the complete sequence of *R. norvegicus* p21 mRNA (NM_080782.3) and detected their affinity to HuR *in vitro*. Several AUUUA pentamers and a U-rich element were recognized in the 3′-UTR of p21 mRNA, as underlined in Fig. 7A. Neither the 5′-UTR nor CR contains similar motifs. Therefore, it is reasonable that HuR binds to p21 mRNA in its 3′-UTR particularly to the representative sequence from position 537 to 809 (3′F), which is abundant with AUUUA motifs. The notion was tested by a pull-down assay and western blot analysis, as described in the "Materials And Methods" section. The DNA templates of the 5′-UTR, CR, 3′-UTR and the selected fragment in 3′-UTR (3′F) with T7 RNA polymerase

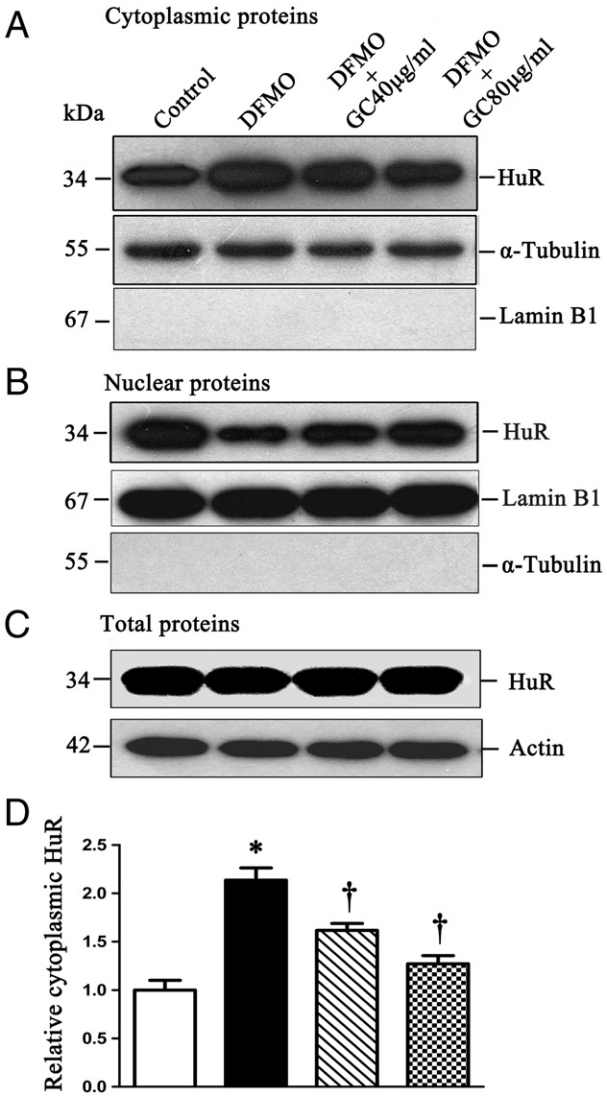

Fig. 5. GC modulated the nucleocytoplasmic distribution of HuR in IEC-6 cells. The levels of cytoplasmic HuR (A), nuclear HuR (B) and HuR in whole-cell lysates (C) were detected by western blot analysis with 50 μg of protein run on 12% gels. To confirm even loading of the samples, alpha-tubulin (55 kDa), lamin B1 (67 kDa) and beta-actin (42 kDa) were used as cytoplasmic, nuclear and whole-cell loading controls, respectively, in each blot for detecting HuR (36 kDa). Alpha-tubulin and lamin B1 were also used to monitor the purity of cytoplasmic and nuclear fractions during protein isolation. (D) Quantitative analysis derived from densitometric scans of immunoblots of cytoplasmic HuR as described in (A). Values are the mean±S.E.M. from three separate experiments. *P<.05 when compared to controls and cells treated with DFMO plus GC. †P<.05 when compared to cells treated with DFMO.

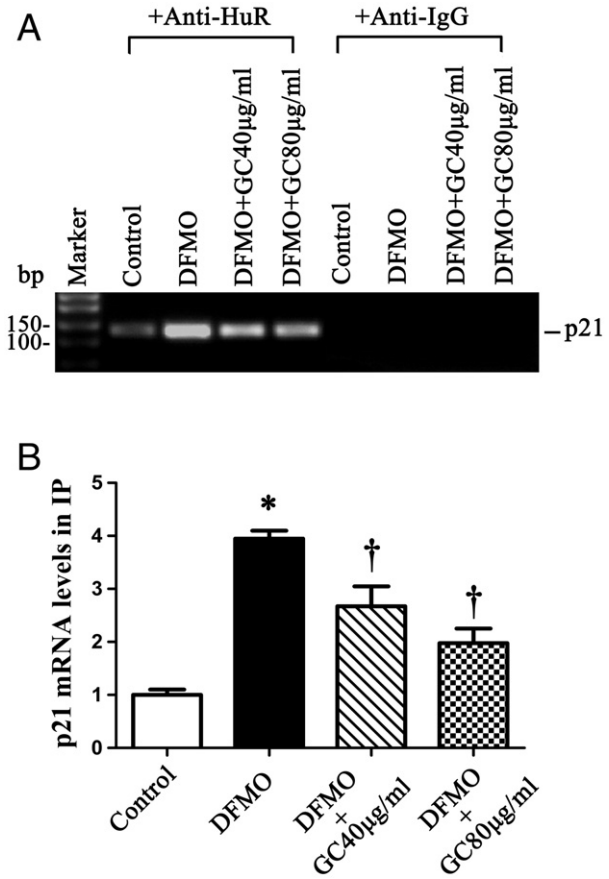

Fig. 6. GC regulates the intracellular location of endogenous HuR-p21 mRNA–mRNP complexes. (A) Messenger RNA–HuR complexes from control cells, cells grown in the presence of DFMO and cells treated with DFMO plus 40 μg/ml or 80 μg/ml GC were specifically immunoprecipitated using anti-HuR antibody. As an internal control, nonspecific IgG1 was used in the same way as anti-HuR antibody in the immunoprecipitation. p21 mRNA extracted from mRNP complexes was amplified by reverse transcription PCR, and amplification products (126 bp) were visualized in agarose gels. (B) Quantitative RT-PCR analysis to assess the level of endogenous p21 mRNA from mRNA–HuR complexes. Values are the mean±S.E.M. of data from three independent experiments. *P<.05 when compared to control cells and cells treated with DFMO plus GC. †P<.05 when compared to cells treated with DFMO.

promoter sequence at their endings were used for synthesizing their corresponding biotinylated mRNA portions. As predicted, the cytoplasmic HuR from untreated IEC cells had a high affinity for the 3′-UTR of p21 mRNA particularly to 3′F, which has the most HuR motifs. However, negative binding was shown in the 5′-UTR and CR sequences (Fig. 7B). Based on the validity of the p21 mRNA 3′-UTR binding to HuR, the highly positive 3′F sequence was used to further bind to cytoplasmic HuR prepared from IEC-6 cells in different groups. DFMO treatment increased the binding intensity of HuR to 3′F in p21 mRNA, but this binding was significantly reduced when cells were treated with 40 μg/ml and 80 μg/ml GC (Fig. 7C). The *in vitro* binding intensity between HuR and p21 mRNA 3′-UTR in each group differs in a similar pattern as the changes in cytoplasmic HuR under the same conditions (Fig. 5A).

Second, whether p21 mRNA 3′-UTR AREs were involved in GC-mediated down-regulation of p21 was tested by cloning the p21 mRNA ARE sequence downstream of a reporter gene coding region and performing a dual-luciferase reporter assay. In Fig. 7D(b), the cloning position of 3′F dsDNA was downstream of the firefly luciferase reporter gene. No changes in the luciferase reporter gene activity were seen in response to DFMO and GC treatment when testing a control construct without the p21 mRNA ARE (Fig. 7E, pGL3-Luc). In contrast, luciferase reporter gene activity was significantly increased by DFMO after transfecting the plasmid bearing the p21 mRNA ARE, whereas with supplementation with 40 μg/ml and 80 μg/ml of GC, the increased translation of the luciferase reporter gene was prevented, as indicated by a decrease in the p21 ARE luciferase reporter gene activity (Fig. 7E, pGL3-Luc-3′F). These results support the view that GC decreases p21 mRNA translation through an ARE within its mRNA 3′-UTR that bears a HuR target motif.

4. Discussion

Licorice is a popular herb that has been used in food and medicines for thousands of years. Its antiulcer and mucosal protective actions

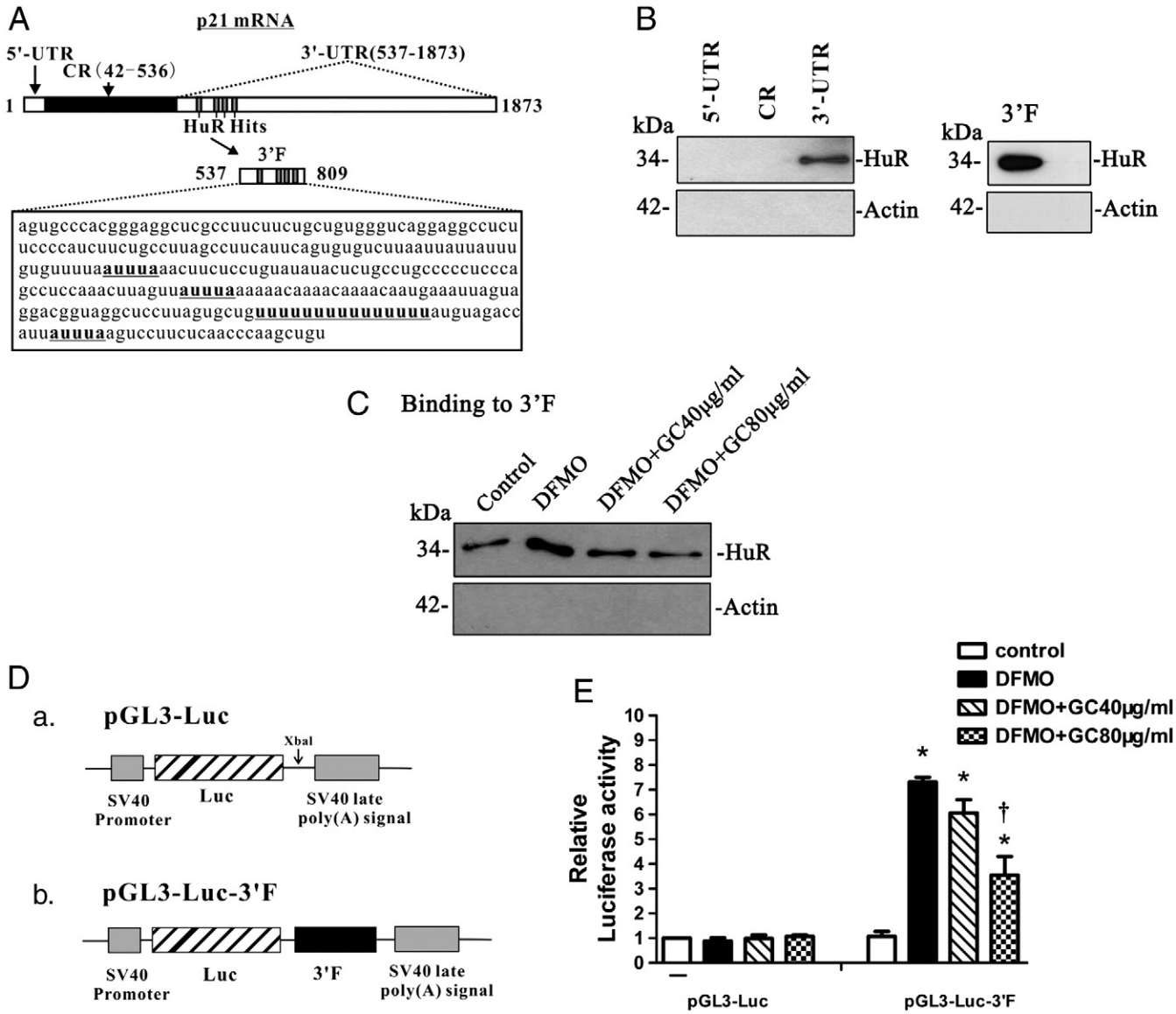

Fig. 7. GC enhanced the expression of the HuR-binding p21 mRNA ARE fragment. (A) Schematic representation of rat p21 mRNA (GenBank accession number: NM_080782.3) and the representative sequence 3′F, which contains AU-rich elements with the AUUUA motif and U-rich element in its 3′-UTR. (B) The diverse binding capacities of the complete 5′-UTR (41 bp), CR (495 bp), 3′-UTR (1337 bp) and 3′F (273 bp) to cytoplasmic HuR from untreated IEC-6 cells were analyzed using a biotin pull-down assay and visualized by western blotting. (C) Changes in binding of the representative fragment in 3′-UTR, 3′F, to the cytoplasmic HuR (120 μg per sample) from control cells, DFMO-treated cells and cells treated with DFMO plus 40 μg/ml and 80 μg/ml GC were shown by a biotin pull-down assay and western blot. (D) Schematic representation of the plasmids: (a) control (pGL3-Luc); (b) chimeric luciferase construct containing the fragment of interest, 3′F, downstream of the reporter gene (pGL3-Luc-3′F). (E) Effect of GC on luciferase reporter activity in IEC-6 cells transfected with the control plasmid pGL3-Luc and chimeric luciferase plasmid pGL3-Luc-3′F. The dual-luciferase reporter assay was performed as described in the "Materials And Methods" section. The ratio of firefly luciferase to the internal control *Renilla* luciferase from control cells cotransfected with the pGL3-Luc and pRL-SV40 vectors was set to 1 (shown by —). Luciferase values were normalized to this negative control to obtain translation efficiencies and were expressed as the mean±S.E.M. of data from three separate experiments. *P<.05 when compared to control cells and cells treated with DFMO plus GC. †P<.05 when compared to cells treated with DFMO.

have been confirmed by numerous clinical trials and animal experiments. Emerging knowledge about the posttranscriptional gene regulatory mechanism of intestinal proliferation provides us a novel framework for exploring the possible molecular basis that underlies mucosa protection by licorice. We investigated the action of licorice on intestinal crypt cell proliferation and the corresponding molecular mechanisms.

We tested our hypothesis in a DFMO-treated IEC-6 cell line. In this study, we demonstrated that the aqueous licorice extract could partially reverse the antiproliferative effect of DFMO on IEC-6 cells in a dose-dependant manner. The impact of licorice on IEC-6 cells correlated with p21. The elevated p21 mRNA and protein levels induced by DFMO were down-regulated with concomitant administration of licorice extract. Moreover, the decrease in p21 expression paralleled the nucleocytoplasmic distribution of HuR, by which p21 mRNA was destabilized when HuR reduced its binding to AU-rich and U-rich elements in the 3′-UTR of p21 mRNA. The effect of licorice on p21 translation through the HuR-targeted ARE fragment from the p21 mRNA 3-'UTR was further studied by the luciferase reporter assay. Considering the fact that lowering endogenous HuR levels through expression of antisense HuR decreased p21 RNA-protein complexes [31], it is reasonable to conclude that licorice converts the DFMO-treated IEC-6 cell cycle back to normal progression by HuR-mediated regulation of p21 mRNA stability and expression. Taken together, this study improves our understanding of the protective action of licorice upon intestinal epithelium at the posttranscriptional level.

A previous study by Ray et al. [19] indicated that the elevation of p21 induced by DFMO paralleled the activation of the MAPK pathway. Hence, it was proposed that DFMO might cause stress and activate stress-regulated kinase, which in turn would increase p21 transcription. Similarly, it was documented that amino acid deprivation could increase p21 mRNA stability [40]. In addition, polyamines are derived from the amino acid ornithine. We presume that the polyamine depletion here may act as a trigger for nutritional stress and promote the expression of p21 mRNA. However, HuR has been proven to function as a posttranscriptional regulator of some mRNAs in normal and stressed cells [41]. For instance, HuR plays a major role in regulating oxidative-stress-induced p21 expression by enhancing p21 mRNA stability when the human RKO cells were exposed to UV light. In glioma cells that underwent amino acid starvation, the stability of Cat-1 mRNA was mediated by its AU-rich elements that bound the cytoplasmic shuttling HuR [42]. These findings resemble the interaction between p21 mRNA and HuR elucidated in our research and offer indirect evidence that HuR-mediated p21 mRNA stabilization is one of the underlying mechanisms in licorice reviving the proliferative capability of IEC-6 cells.

HuR was shown to be a molecular target for licorice in our research. Considering the role of this ubiquitously expressed RNA binding protein in the posttranscriptional regulation of many ARE-containing mRNAs, such as c-myc, p53, p21, bcl-2 and XIAP [41,43,44], it would give us a whole new perspective on possible molecular mechanisms of the pharmacological action of licorice for therapeutic purposes. Furthermore, with a long-term expectation of making a breakthrough in elucidating the complex mechanisms in herbal medicine, we hope the posttranscriptional control of gene expression through RBPs will help us gain novel insight into the governing mechanisms in the simultaneous changes in the expression of multiple genes after herbal administration.

Licorice has been so frequently used in traditional Chinese medicine (TCM) that it almost appears in every ordinary oral decoction. This phenomenon, according to the ancient theory of TCM, is ascribable to the capability of licorice to enhance the activity of other ingredients in the prescription. However, whether there is a common mechanism that accounts for the versatile properties of licorice in TCM still remains unclear. Most oral drugs are absorbed primarily in the small intestine because the small intestine has the largest absorptive surface in gastrointestinal tract and its membrane is more permeable for drug diffusion [45]. We propose that the frequent use of licorice in TCM may potentially depend, at least partially, on its efficiency in accelerating the synthesis or recovery of intestinal mucosa to sustain sufficient absorptive area.

In summary, concomitant administration of licorice extract could restore the proliferative potential in DFMO-treated IEC-6 cells by down-regulating the level of p21 mRNA. The changes in p21 mRNA were coupled with the cytoplasmic accumulation of HuR. HuR stabilized p21 mRNA through AU-rich and U-rich elements in the 3′-UTR, whereas licorice destabilized p21 mRNA by decreasing the cytoplasmic shuttling of HuR and in turn returned the cell cycle back to normal progression. This study suggests that licorice exerts its proproliferative action on the intestinal crypt cells at the molecular level and is also the first report that licorice can posttranscriptionally regulate mRNA expression through an RNA-binding protein.

Supplementary materials related to this article can be found online at doi:10.1016/j.jnutbio.2011.07.009.

Acknowledgments

This research was supported by a grant from Natural Science Foundation of Guangdong Province, China (Grant 10151040701000051). We are extremely grateful to Dr. Jian-Ying Wang, who is the Associate Chair for Basic Research in Departments of Surgery and Pathology, University of Maryland School of Medicine, for his generosity in providing expert technical guidance and assistance.

References

[1] Fiore C, Eisenhut M, Ragazzi E, Zanchin G, Armanini D. A history of the therapeutic use of liquorice in Europe. J Ethnopharmacol 2005;99:317–24.
[2] Obolentseva G, Litvinenko V, Ammosov A, Popova T, Sampiev A. Pharmacological and therapeutic properties of licorice preparations (a review). Pharm Chem J 1999;33:427–34.
[3] Fintelmann V. Modern phytotherapy and its uses in gastrointestinal conditions. Planta Med 1991;57:S48–52.
[4] Martin MD, Sherman J, van der Ven P, Burgess J. A controlled trial of a dissolving oral patch concerning glycyrrhiza (licorice) herbal extract for the treatment of aphthous ulcers. Gen Dent 2008;56:206–10 quiz 11-2, 24.
[5] Oloumi MM, Derakhshanfar A, Nikpour A. Healing potential of liquorice root extract on dermal wounds in rats. J Vet Res 2007;62:147–54.
[6] Revers FE. Licorice juice in therapy of ventricular and duodenal ulcers. Ned Tijdschr Geneeskd 1948;92:2968–73.
[7] Blumenthal M, Goldberg A, Brinckmann J, Foster S. Herbal medicine — expanded Commission E monographs. Austin (Tex): American Botanical Council; 2000.
[8] Dai S, Ogle CW, Cho CH. Effects of carbenoxolone sodium on gastric and duodenal mucus synthesis in mice. Pharmacology 1986;33:58–60.
[9] van Marle J, Aarsen PN, Lind A, van Weeren-Kramer J. Deglycyrrhizinised liquorice (DGL) and the renewal of rat stomach epithelium. Eur J Pharmacol 1981;72: 219–25.
[10] Mammen JM, Matthews JB. Mucosal repair in the gastrointestinal tract. Crit Care Med 2003;31:S532–7.
[11] Barker N, van de Wetering M, Clevers H. The intestinal stem cell. Genes Dev 2008;22:1856–64.
[12] Daniele B, D'Agostino L. Proliferation and differentiation of the small intestinal epithelium: from Petri dish to bedside. Ital J Gastroenterol 1994;26:459–70.
[13] Dignass AU. Mechanisms and modulation of intestinal epithelial repair. Inflamm Bowel Dis 2001;7:68–77.
[14] Zhang Z, Chen W. Effects of extracts from *Codonopsis pilosula*, *Astragalus membranaceus*, *Atractylodes macrocephala* and *Glycyrrhiza uralensis* on intestinal crypt cells proliferation. Pharmacol Clin Chin Mater Med 2002;18:10–2.
[15] Quaroni A, Wands J, Trelstad RL, Isselbacher KJ. Epithelioid cell cultures from rat small intestine. Characterization by morphologic and immunologic criteria. J Cell Biol 1979;80:248–65.
[16] Wang JY, Johnson LR. Luminal polyamines stimulate repair of gastric mucosal stress ulcers. Am J Physiol 1990;259:G584–92.
[17] Wang JY, Johnson LR. Polyamines and ornithine decarboxylase during repair of duodenal mucosa after stress in rats. Gastroenterology 1991;100:333–43.
[18] Capano G, Bloch KJ, Carter EA, Dascoli JA, Schoenfeld D, Harmatz PR. Polyamines in human and rat milk influence intestinal cell growth in vitro. J Pediatr Gastroenterol Nutr 1998;27:281–6.
[19] Ray RM, Zimmerman BJ, McCormack SA, Patel TB, Johnson LR. Polyamine depletion arrests cell cycle and induces inhibitors p21(Waf1/Cip1), p27(Kip1), and p53 in IEC-6 cells. Am J Physiol 1999;276:C684–91.
[20] Wang JY, McCormack SA, Viar MJ, Wang H, Tzen CY, Scott RE, et al. Decreased expression of protooncogenes c-fos, c-myc, and c-jun following polyamine depletion in IEC-6 cells. Am J Physiol 1993;265:G331–8.
[21] Li L, Liu L, Rao JN, Esmaili A, Strauch ED, Bass BL, et al. JunD stabilization results in inhibition of normal intestinal epithelial cell growth through P21 after polyamine depletion. Gastroenterology 2002;123:764–79.
[22] Patel AR, Li J, Bass BL, Wang JY. Expression of the transforming growth factor-beta gene during growth inhibition following polyamine depletion. Am J Physiol 1998;275:C590–8.
[23] Keene JD. RNA regulons: coordination of post-transcriptional events. Nat Rev Genet 2007;8:533–43.
[24] Glisovic T, Bachorik JL, Yong J, Dreyfuss G. RNA-binding proteins and post-transcriptional gene regulation. FEBS Lett 2008;582:1977–86.
[25] Zou T, Mazan-Mamczarz K, Rao JN, Liu L, Marasa BS, Zhang AH, et al. Polyamine depletion increases cytoplasmic levels of RNA-binding protein HuR leading to stabilization of nucleophosmin and p53 mRNAs. J Biol Chem 2006;281:19387–94.
[26] Wang JY. Polyamines and mRNA stability in regulation of intestinal mucosal growth. Amino Acids 2007;33:241–52.
[27] Peng SS, Chen CY, Xu N, Shyu AB. RNA stabilization by the AU-rich element binding protein, HuR, an ELAV protein. EMBO J 1998;17:3461–70.
[28] Wang W, Caldwell MC, Lin S, Furneaux H, Gorospe M. HuR regulates cyclin A and cyclin B1 mRNA stability during cell proliferation. EMBO J 2000;19:2340–50.
[29] Ma WJ, Chung S, Furneaux H. The Elav-like proteins bind to AU-rich elements and to the poly(A) tail of mRNA. Nucleic Acids Res 1997;25:3564–9.
[30] Mazan-Mamczarz K, Galban S, Lopez de Silanes I, Martindale JL, Atasoy U, Keene JD, et al. RNA-binding protein HuR enhances p53 translation in response to ultraviolet light irradiation. Proc Natl Acad Sci U S A 2003;100:8354–9.
[31] Wang W, Furneaux H, Cheng H, Caldwell MC, Hutter D, Liu Y, et al. HuR regulates p21 mRNA stabilization by UV light. Mol Cell Biol 2000;20:760–9.
[32] Commission CP. Pharmacopoeia of the People's Republic of China. 8 ed. Beijing: Chemical Industry Press; 2005.

[33] Zou T, Rao JN, Liu L, Marasa BS, Keledjian KM, Zhang AH, et al. Polyamine depletion induces nucleophosmin modulating stability and transcriptional activity of p53 in intestinal epithelial cells. Am J Physiol Cell Physiol 2005;289:C686–96.
[34] Laemmli UK. Cleavage of structural proteins during the assembly of the head of bacteriophage T4. Nature 1970;227:680–5.
[35] Lopez de Silanes I, Zhan M, Lal A, Yang X, Gorospe M. Identification of a target RNA motif for RNA-binding protein HuR. Proc Natl Acad Sci U S A 2004;101:2987–92.
[36] Gartel AL, Serfas MS, Tyner AL. p21-negative regulator of the cell cycle. Proc Soc Exp Biol Med 1996;213:138–49.
[37] Ray RM, McCormack SA, Johnson LR. Polyamine depletion arrests growth of IEC-6 and Caco-2 cells by different mechanisms. Am J Physiol Gastrointest Liver Physiol 2001;281:G37–43.
[38] Guhaniyogi J, Brewer G. Regulation of mRNA stability in mammalian cells. Gene 2001;265:11–23.
[39] Fan XC, Steitz JA. HNS, a nuclear-cytoplasmic shuttling sequence in HuR. Proc Natl Acad Sci U S A 1998;95:15293–8.
[40] Leung-Pineda V, Pan Y, Chen H, Kilberg MS. Induction of p21 and p27 expression by amino acid deprivation of HepG2 human hepatoma cells involves mRNA stabilization. Biochem J 2004;379:79–88.
[41] CM B JAS. HuR and mRNA stability. Cell Mol Life Sci 2001;58:266–77.
[42] Yaman I, Fernandez J, Sarkar B, Schneider RJ, Snider MD, Nagy LE, et al. Nutritional control of mRNA stability is mediated by a conserved AU-rich element that binds the cytoplasmic shuttling protein HuR. J Biol Chem 2002; 277:41539–46.
[43] Ghisolfi L, Calastretti A, Franzi S, Canti G, Donnini M, Capaccioli S, et al. B cell lymphoma (Bcl)-2 protein is the major determinant in bcl-2 adenine-uridine-rich element turnover overcoming HuR activity. J Biol Chem 2009;284:20946–55.
[44] Zhang X, Zou T, Rao JN, Liu L, Xiao L, Wang PY, et al. Stabilization of XIAP mRNA through the RNA binding protein HuR regulated by cellular polyamines. Nucleic Acids Res 2009;37:7623–37.
[45] Beers MH. The Merck manual. 18th ed. Whitehouse Station: Merck research laboratories; 2006.